

Mathematical Modelling of p53 Signalling in Response to DNA Damage

Michelle Feng & Graeme Ko

AMATH/BIOL 382

Brian Ingalls

April 15, 2022

Abstract	2
1.0 Introduction	2
1.1 Overview of gene regulatory networks (GRNs)	2
1.2 p53's role in molecular oncology	2
1.3 Motivation for mathematical modelling of p53 response	3
2.0 Model	4
2.1 Model summary	4
2.2 Model implementation	5
2.3 Model limitations	6
3.0 Compartmental model	6
3.1 Model summary	6
3.2 Model assumptions	7
3.3 Model results	10
4.0 Extension	11
4.1 Extension motivation and setup.....	11
4.2 Extension results	12
5.0 Conclusion and future considerations	12
References.....	13
Appendix A: Model parameters and equations for spatial model.....	14
Appendix B: Compartmental Model Parameters.....	17

Abstract

Since its discovery over 40 years ago, p53 has been a greatly studied subject of interest within the field of mathematical biology. P53 is a gene which plays a key role in the regulation of cell division and cell death. Mutations within p53 lead to cancerous phenotypes, thus it is important to understand the underlying genetic mechanisms within the p53 pathway. A particular interest in the study of p53 is to model its oscillatory behaviour in response to DNA damage. Elias and Macnamara (2021) examine several approaches into simulated models that represent the oscillatory dynamics, exploring time delay models, spatial models, and coupled negative-positive feedback models. In this report, we specifically investigate a spatial compartmental model which separates the nucleus and cytoplasm of the cell into different domains. The compartmental model focuses on protein interactions and transport of p53, Mdm2, ATM, and Wip1, ultimately achieving the expected oscillatory behaviour. Further analysis of the model shows that a lack of Wip1 phosphatase activity increases active p53 concentration. Therefore, it is relevant for modelling Wip1 inhibiting drugs that have been seen to promote cancer cell death through the p53 pathway.

1.0 Introduction

1.1 Overview of gene regulatory networks (GRNs)

Gene regulatory networks are used to mathematically describe a collection of genetic molecules that interact with each other (Emmert-Streib et al., 2014). Interactions affect changes to the transcription and production of molecules through either activation or inhibition mechanisms. Since each gene can have multiple regulators, expression levels can be represented as functions with multiple inputs. This property allows for great freedom when designing feedback networks. GRNs are found across all cellular mechanisms and processes, and are therefore an important resource when investigating cell behaviour. Most importantly, GRNs are a vitally important tool in understanding what happens on a genetic level when cells deviate from their typical behaviour, such as on the onset of cancer.

1.2 p53's role in molecular oncology

P53 is a key player in molecular oncology, and acts as a tumour suppression protein. There are many regulatory functions of p53; specifically, its main role in healthy cells is to suppress changes to a cancerous phenotype by acting as a gatekeeper of key cellular processes such as apoptosis, DNA damage repair, senescence, and cell cycle arrest (Boyd & Vlatkovic,

2008). It is often referred to as the guardian of the genome. P53 is the most frequently mutated gene in cancer, and loss of p53 function has shown to promote cancer in both humans and model systems. Over the last 20 years, there have been many mathematical efforts into modelling the p53 genetic pathway. Many extra and intra-cellular stresses, such as heat, DNA damage, and hypoxia activate p53. The subsequent behaviour and downstream effects depend on the nature of the stress. Stress is detected by a range of enzymes which signal p53 through the promotion of post-translational modifications, such as phosphorylation, acetylation, and methylation (Boyd & Vlatkovic, 2008). Although the coordination process of modifications are not yet completely understood, modifications to p53 results in both upregulation of p53 protein, as well as the stimulation of p53 transcriptional activation.

Most experiments have focused on the activation of p53 by irradiation, which causes DNA double stranded breaks. This leads to a downstream reaction of the phosphorylation of p53 which interrupts its binding to its main antagonist Mdm2 and results in an increase in p53. Subsequent dynamical behaviour of p53 has been the focus of most studies.

1.3 Motivation for model development

In many genetic pathways, a key feature is the periodic or fluctuating expression of proteins. However, as p53's biological role as a cellular gatekeeper, its levels will naturally fluctuate from cell to cell. Therefore it is more meaningful to investigate the protein expression within individual cells. Analysis of immunoblots at the cell population level have shown that p53 and Mdm2 undergo damped oscillations following significant DNA damage, and the amplitude of oscillations is directly correlated to the amount of DNA damage (Elias & Macnamara, 2021).

Batchelor et al. determined that sustained oscillations (with fixed amplitude and period) could be observed at a single cell level after gamma-irradiation (Batchelor et al., 2011). In this experiment, the number of periods of p53 was directly correlated to the amount of DNA damage and the amplitudes were constant. They hypothesised that these sustained pulses last until either the damage is repaired or the cell dies. The sources of irradiation (gamma or UV) can alter the dynamics exhibited by p53 (periodic or sustained expression), and these p53 dynamics affect the outcome of the cell (repair or death).

From existing studies, we can see that the dynamical behaviour of p53 is an important part of its function. It is useful to investigate the mechanisms within its pathway to determine what drives its periodic and sustained expression, and what factors account for the switch between the two states. Therefore, determining mechanisms which provoke oscillations in p53 GRN systems has been a major focus in mathematical modelling. A common feature of GRNs is negative feedback, and this has long been thought to produce oscillations. P53 is regulated, in part, by a negative feedback loop.

2.0 Model

2.1 Model summary

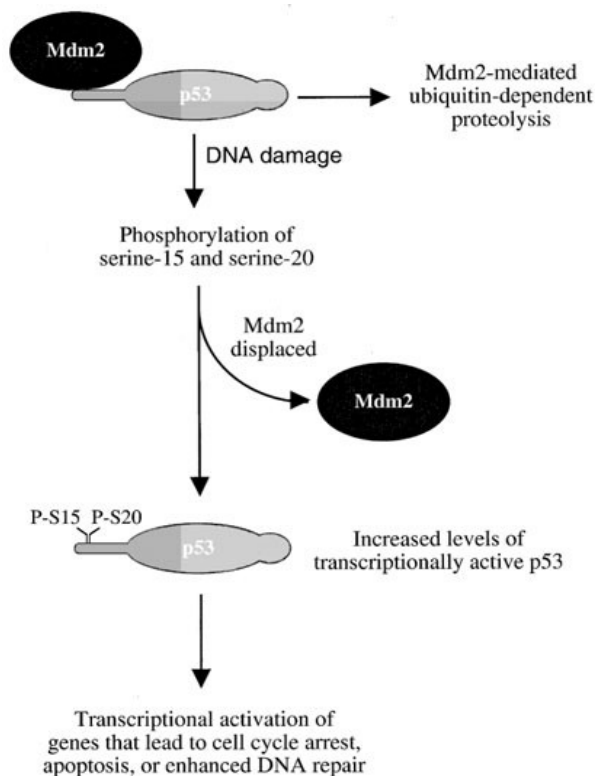


Figure 1. Scheme of the p53-Mdm2 pathway

Source: Lakin & Jackson, 1999

In the p53-Mdm2 pathway, negative feedback occurs through interaction with Mdm2; Mdm2 represses the transcriptional activity of p53 by binding to and ubiquitinating it, which marks it for degradation. Mdm2 repression of p53 is important in processes such as wound healing, but if levels of Mdm2 are too high and repression is too strong, this can contribute to tumour formation, thus Mdm2 is referred to as an oncogene. Activated p53 induces transcription of Mdm2 by binding to its promoter. As the amount of p53 increases, binding and upregulation of Mdm2 increases, and as the amount of Mdm2 increases, binding and down-regulation of p53 increases.

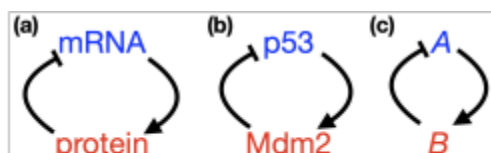


Figure 2. Scheme representing simplistic negative feedback systems

Source: Elias & Macnamara, 2021

2.2 Model implementation

For the simplest implementation of the negative feedback model of the p53-Mdm2 pathway, a pair of rate equations for the concentration of p53 (denoted by x) and the concentration of Mdm2 (denoted by y) were chosen. The system of Ordinary Differential Equations (ODEs) is as follows:

$$\dot{x}(t) = k_s - k_1 y(t) \frac{x(t)}{K_1 + x(t)} - d_x x(t),$$

$$\dot{y}(t) = k_2 \frac{x(t)^n}{K_2^n + x(t)^n} - d_y y(t).$$

P53 is produced at a constant rate of k_s , and degraded either in an Mdm2-dependent manner (modelled by a Michaelis-Menten function) or independently of Mdm2 with the rate of degradation, d_x . Mdm2 is produced at a rate which depends on the concentration of p53 (modelled by a Hill function with coefficient n) and degraded at a rate of d_y . All solution trajectories (x, y) , regardless of initial conditions, converge eventually to a single positive steady state (fixed point), and located where the curves $\dot{x}(t) = \dot{y}(t) = 0$. The steady state is located where the curves (nullclines) intersect.

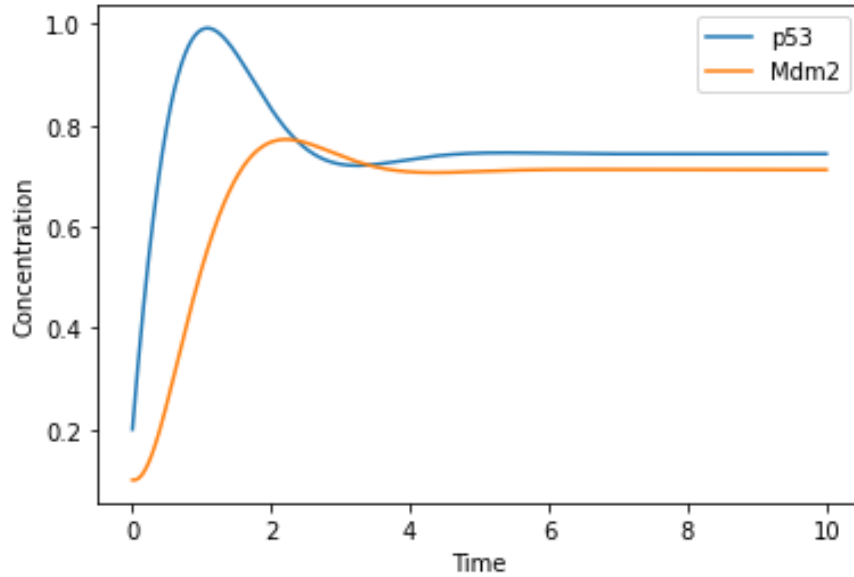


Figure 3. Simulated solution of ODE system, starting from $(0.2, 0.1)$ at $t = 0$

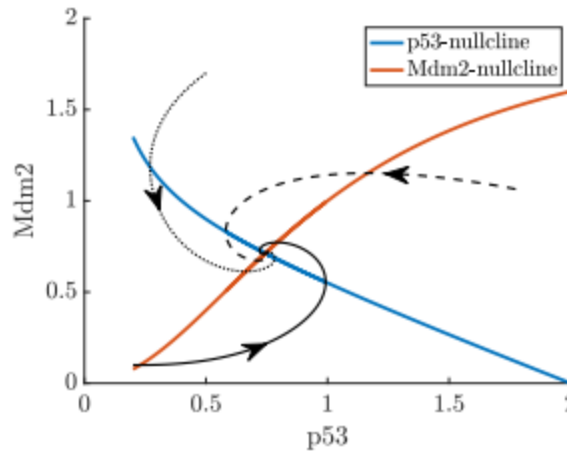


Figure 4. Three trajectories and nullclines in the p53-Mdm2 phase plane.

Source: Elias & Macnamara, 2021

2.3 Model limitations

Early GRN modelling using ODEs showed that the presence of negative feedback alone was insufficient to produce fluctuating protein levels. From stability analysis, it has been shown that an intermediary is required to push GRNs with simple negative feedback from stable fixed points (sustained expression) to a stable limit cycle (periodic fluctuations). These intermediaries may be the time taken for molecular processes to occur (time delay), the requirement for molecules to move to certain locations within a cell (spatial effects), or additional interactions with other molecules (positive feedback) (Elias & Macnamara, 2021).

In addition to the fact that negative feedback alone is insufficient to provoke stable oscillatory behaviour, the simple two-gene GRN between p53 and Mdm2 is a simplification of the highly complex genetic pathway which exists. Thus, it is important to incorporate further aspects of the p53 pathway to model the biological dynamics accurately.

3.0 Compartmental model

3.1 Model summary

For the purpose of finding a model of p53 that supports oscillatory behaviour after DNA double strand breaks, a compartmental model was explored based on the work of Elias et al.

(2014). This model focuses on a single cell and separates the nucleus and cytoplasm of the cell into different domains. A system of ordinary differential equations is used to model the interactions and transport between cell domains of key proteins and mRNA in the p53 regulatory network.

In addition to p53 and Mdm2, the behaviour of proteins ATM and Wip1 will also be included into the model. ATM is a dimer in its inactive form, and once DNA damage occurs it is likely activated through being able to sense changes to the chromatin structure and subsequent induced chemical reactions. Following the damage, ATM quickly converts to its active form by dissociating into monomers. Once activated, ATM can in turn activate p53 through phosphorylation which prevents p53 from binding to Mdm2. When p53 interacts with DNA, it will enable the transcription of more Mdm2 and Wip1. Wip1 is a phosphatase which can deactivate ATM or p53 through dephosphorylation. After dephosphorylation, p53 will again be susceptible to binding with Mdm2 and being ubiquitinated. Therefore, both Mdm2 and Wip1 act in a negative feedback loop with p53 as seen in Figure 5. (Elias et al., 2014).

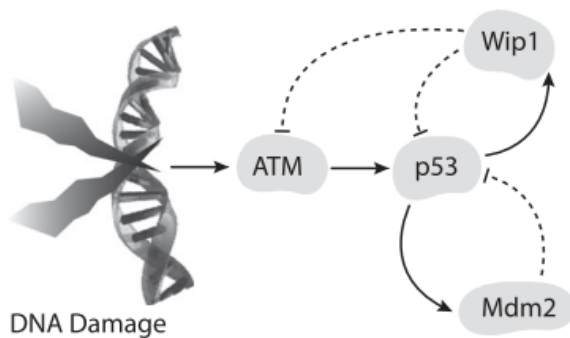


Figure 5. Extended p53 regulatory network
Source: Elias et al., 2014

3.2 Model assumptions

This section will outline assumptions made in the model and explain the choices for some key parameters and equation terms. Descriptions and values of the parameters used can be found in Appendix B. The system of equations which we solved using python can be seen in Table 1.

Table 1: Compartmental Equations

$\frac{du_0}{dt} = k_{dph1}u_5\frac{u_3}{K_{dph1}+u_3} - k_1u_1\frac{u_0}{K_1+u_0} - k_{ph1}u_4\frac{u_0}{K_{ph1}+u_0} - p_0V_r(u_0 - v_0)$	$\frac{dv_0}{dt} = k_s - k_1v_1\frac{v_0}{K_1+v_0} - p_0(v_0 - u_0) - \delta_0v_0$
$\frac{du_1}{dt} = -p_1V_r(u_1 - v_1) - \delta_1u_1$	$\frac{dv_1}{dt} = k_{tm}v_2 - p_1(v_1 - u_1) - \delta_1v_1$
$\frac{du_2}{dt} = k_{Sm} + k_{spm}\frac{u_3^4}{K_{spm}^4 + u_3^4} - p_2V_ru_2 - \delta_2u_2$	$\frac{dv_2}{dt} = p_2u_2 - k_{tm}v_2 - \delta_2v_2$
$\frac{du_3}{dt} = k_{ph1}u_4\frac{u_0}{K_{ph1}+u_0} - k_{dph1}u_5\frac{u_3}{K_{dph1}+u_3}$	$\frac{dv_3}{dt} = 0$
$\frac{du_4}{dt} = k_{ph2}E\frac{ATM_{TOT} - u_4}{K_{ph2} + \frac{1}{2}(ATM_{TOT} - u_4)} - 2k_{dph2}u_5\frac{u_4^2}{K_{dph2} + u_4^2}$	$\frac{dv_4}{dt} = 0$
$\frac{du_5}{dt} = p_5V_ru_5 - \delta_5u_5$	$\frac{dv_5}{dt} = k_{tw}v_6 - p_5v_5 - \delta_5v_5$
$\frac{du_6}{dt} = k_{sw} + k_{spw}\frac{u_3^4}{K_{spw}^4 + u_3^4} - p_6V_ru_6 - \delta_6u_6$	$\frac{dv_6}{dt} = p_6u_6 - k_{tw}v_6 - \delta_6v_6$

The ‘u’ variables denote a concentration in the nucleus and the ‘v’ variables denote a concentration in the cytoplasm. The molecule that each ‘u’ and ‘v’ variable represent are listed here:

$$\begin{aligned} u_0 &= [p53]^{(n)}, u_1 = [Mdm2]^{(n)}, u_2 = [Mdm2_{mRNA}]^{(n)}, \\ u_3 &= [p53_p]^{(n)}, u_4 = [ATM_p]^{(n)}, u_5 = [Wip1]^{(n)}, \\ u_6 &= [Wip1_{mRNA}]^{(n)}, v_0 = [p53]^{(c)}, v_1 = [Mdm2]^{(c)}, \\ v_2 &= [Mdm2_{mRNA}]^{(c)}, v_3 = [p53_p]^{(c)}, v_4 = [ATM_p]^{(c)}, \\ v_5 &= [Wip1]^{(c)}, v_6 = [Wip1_{mRNA}]^{(c)} \end{aligned}$$

where the superscript denotes whether it describes cytoplasmic (c) or nuclear (n) concentrations. A ‘p’ subscript is for proteins that have been phosphorylated and thus are in their active form.

The variable ‘E’ denotes a hypothetical molecule which activates ATM following DNA damage. Therefore, higher E values correspond to a higher severity of DNA damage. V_r is a special volume ratio which accounts for the difference in average reaction rate between the nucleus and cytoplasm based on their relative volumes. The permeability value of p53 was based

on experimental data. However, the permeability changes depending on the N-mer configuration of p53 proteins. Thus, p53 permeability was taken as an averaged value from the different possible configurations. The permeability of other molecules such as Wip1 was estimated based on the permeability of other well known molecules of similar weights. Elias et al. (2014) state that most model parameters were taken from experimental data when possible, but some were chosen to ensure oscillatory behaviour.

Most of the equations make use of Michaelis-Menten kinetics arising from quasi-steady state approximations being applied to phosphorylation and ubiquitination interactions. For the equations that depict active p53 transcribing more Mdm2 or Wip1, a hill function with a coefficient of 4 is used. This is because when p53 interacts with DNA it is preferentially in a tetramer configuration (Elias et al., 2014). The transport terms in the equations depend on the permeability 'p', the special volume ratio ' V_r ', and the difference in concentration of the molecule between the nuclear and cytoplasmic domains. Other constant terms also appear in the equations due to basal rates of transcription and degradation.

It will be assumed that inactivated p53 is free to move between compartments after being translated at a basal rate in the cytoplasm. However, the activated version of p53 which forms tetramers will not be free to cross from the nucleus into the cytoplasm. Although p53 degradation is controlled primarily by Mdm2, there will also be a natural degradation rate of p53 in the cytoplasm. Mdm2 is expected to have free migration between compartments and can ubiquitinate inactive p53 in both domains. Wip1 is primarily found in the nucleus, and therefore the model will assume that after it is translated in the cytoplasm it migrates into the nucleus to perform its function. Both Wip1 and Mdm2 are assumed to only be degraded by a constant basal rate. ATM is a heavy protein, and therefore the model assumes that it will not be transported across compartments and that degradation or production of ATM will be irrelevant. Instead, the total ATM concentration is set as constant but it will switch between its active or inactive state in the nucleus. Activated ATM only exists within the nucleus, and therefore ATM in the cytoplasm will have no effect on p53 activation. This is reflected by the system equations where the rate of activated p53 and ATM are set as 0 within the cytoplasm.

This ODE model does not evaluate spatial concentration gradients within individual compartments, meaning that the concentration of a protein is set as constant throughout the entire domain and transport is only considered across domains. When solving the systems of equations, the initial parameters were set to zero given the assumptions that p53 levels are thought to be low in unstressed cells and that the model will reach a stable limit cycle.

3.3 Model results

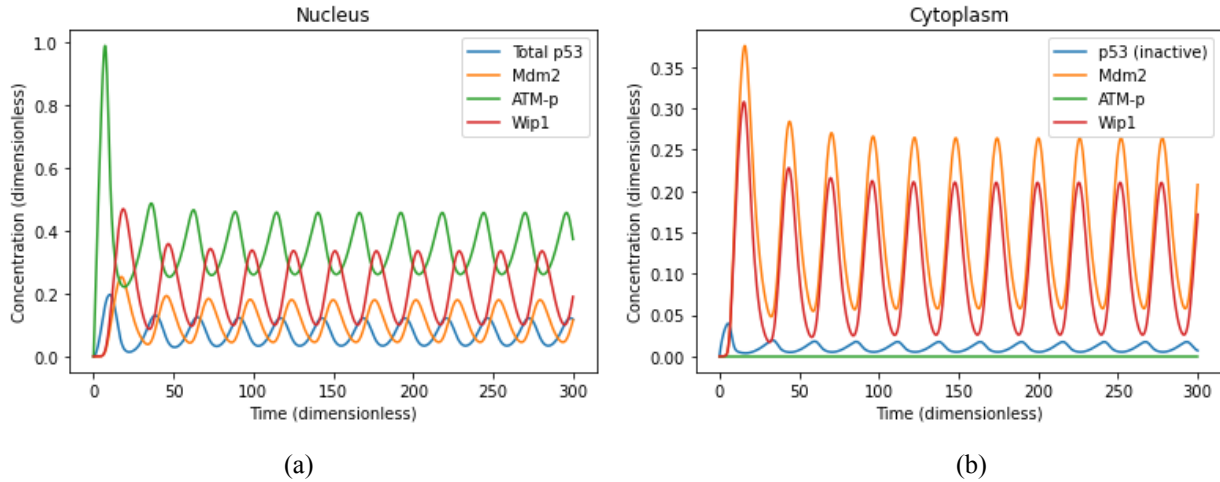


Figure 6. Protein concentrations in the (a) nucleus and (b) cytoplasm

Figure 6 shows a graphical representation of the solved compartmental model. A damage parameter of $E=0.1\mu\text{M}$ was used in the simulation. As expected, oscillatory behaviour with fixed amplitude was achieved. The high amplitude of the first peak has little significance in the context of the overall behaviour. Phase differences between peaks of different protein concentrations in the nucleus behave as expected. Figure 6a shows that the peak of p53 follows after the peak of activated ATM since high levels of activated ATM will in turn activate p53. The peaks of Mdm2 and Wip1 also follow slightly after the peak of p53 since activated p53 will upregulate the transcription of those proteins. Although the behaviour is very similar, the only major difference between our results and the results of Elias et al. (2014) is that the amplitude of p53 concentration is lower in our simulation. Since it is just a difference of amplitude, perhaps this indicates that some constant or equation term was incorrectly copied into our code, though we were unable to locate the source of the error.

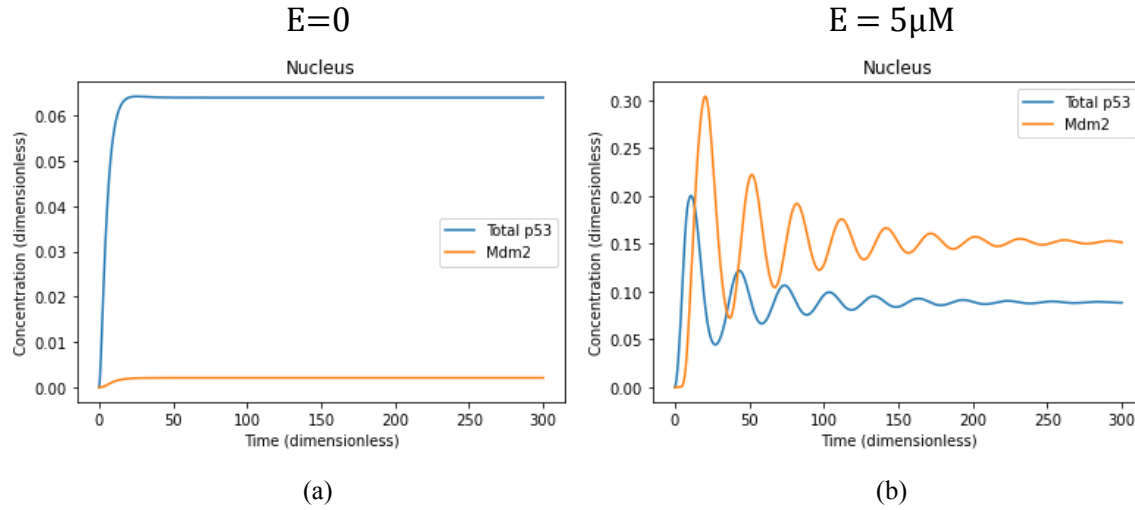


Figure 7. Simulation with varied damage parameters of (a) $E=0$ and (b) $E=5\mu\text{M}$

Figure 7 shows what happens to p53 and Mdm2 when we vary the damage parameter ‘E’ of our compartmental model. When we set $E=0$ the system approaches a steady state and exhibits no oscillatory behaviour. This is to be expected since $E=0$ represents a system with no DNA damage and we already know that oscillations are not seen in unstressed cells. When we increase the damage parameter from the original $0.1\mu\text{M}$ to a more extreme value of $5\mu\text{M}$ we can see the model start to break down. The oscillations become damped and reach a steady state, whereas for a single cell we would expect the oscillations to reach a fixed amplitude. The model could perhaps become more robust for high damage values if extra delays were introduced into the system.

4.0 Extension

4.1 Extension motivation and setup

Since Wip1 deactivates p53 and ATM, we expect to see an increase in p53 activity following Wip1 inhibition. In a study by Pecháčková et al. (2017) they found that a compound called GSK2830371 showed potential for selective inhibition of Wip1 and that it promoted cancer cell death or deterred its growth in combination with chemotherapy and other treatments. Therefore, we wanted to see what happens in our simulation when Wip1 activity is inhibited and if it behaves as expected. To accomplish this, we took the original compartmental model then set the parameters k_{dph1} and k_{dph2} (which represent the dephosphorylation velocity of Wip1 acting on activated ATM and p53) to 0.

4.2 Extension results

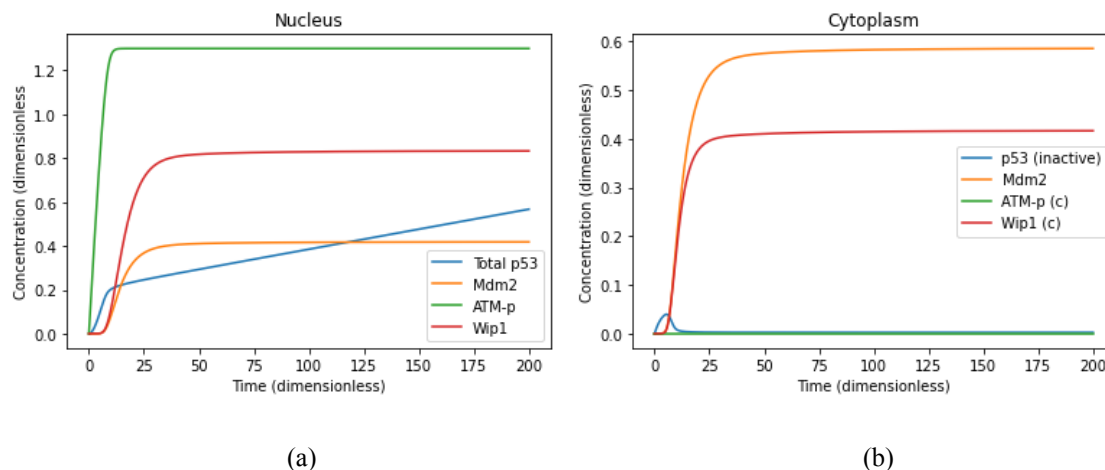


Figure 8. Compartmental model of the (a) nucleus and (b) cytoplasm without phosphatase activity from Wip1

In Figure 8a we see most proteins in the system reach a steady state without the influence of Wip1 activity. However, the concentration of p53 diverges from a steady state solution and instead keeps increasing linearly. This is somewhat expected since Mdm2 can't ubiquitinate activated p53 without the help of Wip1 in our model. Therefore, activated p53 concentration will steadily increase as long as there is active ATM or damage present. While our model extension shows p53 concentration increasing to infinity, a real cell would be expected to increase p53 until either the DNA is repaired or the p53 pathway induces apoptosis.

5.0 Conclusions and future considerations

The p53 regulatory network was first modelled as a simple negative feedback loop between p53 and Mdm2. However, it was found that this model was insufficient to induce the oscillatory behaviour that occurs following DNA damage. A more complex compartmental model had to be used which split the nucleus and cytoplasm into two separate domains that some proteins could be transported across. The compartmental model also included interactions from ATM and Wip1. Model simulations showed the expected relationship between protein concentrations while also achieving oscillatory behaviour. A damage parameter of $E=0$ showed steady state behaviour as expected of a cell with no DNA damage. Our model however was not robust for high values of E where the oscillations become damped over time. We extended the model by removing the phosphatase behaviour from Wip1. This change led to an increase of p53 relative to other protein concentrations. Therefore, the augmented p53 pathway is expected to promote cell cycle arrest or cancer cell death as seen in studies with Wip1 inhibiting compounds.

The model could be further enhanced by accounting for spatial effects on concentration gradients within individual compartments. Our ODE model assumed each concentration to be

evenly distributed within each compartment, whereas a partial differential equation model that accounts for spatial variables would potentially have more success in modelling the transport of proteins or irregularly shaped cells. It could also help make the model more robust to high damage parameters by introducing extra delays from protein translation occurring in the endoplasmic reticulum and not just the cytoplasm. Bifurcation analysis could be performed on the damage parameter to determine at what point the system changes from steady state to oscillatory behaviour. However, more work should be done in relating the damage parameter scale to actual experimental damage data as well. Finally, a stochastic model could be made which takes the model and unique initial values of individual cells then applies it in the context of a population of cells.

References

- Batchelor, E., Loewer, A., Mock, C., & Lahav, G. (2011). Stimulus-dependent dynamics of p53 in single cells. *Molecular Systems Biology*, 7(1), 488. doi:10.1038/msb.2011.20
- Boyd, M. T., & Vlatkovic, N. (2008). P53: A molecular marker for the detection of cancer. *Expert Opinion on Medical Diagnostics*, 2(9), 1013-1024. doi:10.1517/17530059.2.9.1013
- Eliaš, J., Dimitrio, L., Clairambault, J., & Natalini, R. (2014). The dynamics of p53 in single cells: physiologically based ODE and reaction–diffusion PDE models. *Physical biology*, 11(4), 045001.
- Eliaš, J., & Macnamara, C. K. (2021). Mathematical modelling of p53 signalling during DNA damage response: A survey. *International Journal of Molecular Sciences*, 22(19), 10590. doi:10.3390/ijms221910590
- Emmert-Streib, F., Dehmer, M., & Haibe-Kains, B. (2014). Gene regulatory networks and their applications: Understanding biological and medical problems in terms of networks. *Frontiers in Cell and Developmental Biology*, 2. doi:10.3389/fcell.2014.00038
- Lakin, N. D., Jackson, S. P. (1999). Regulation of p53 in response to DNA damage. *Oncogene* 18, 7644-7655. doi:10.1038/sj.onc.1203015
- Pecháčková, S., Burdová, K., & Macurek, L. (2017). WIP1 phosphatase as pharmacological target in cancer therapy. *Journal of molecular medicine (Berlin, Germany)*, 95(6), 589–599. <https://doi.org/10.1007/s00109-017-1536-2>

Appendix A: Simulation Code for Compartmental Model

Code to simulate the Spatial Model, based on p53-Mdm2 negative feedback loop with diffusion model as described by Elias & Macnamara, 2021

```
import numpy as np
from scipy.integrate import odeint
import matplotlib.pyplot as plt
#BIOL 382 Project - ODE Spatial Model

#Parameters
kdph1 = 78 #min-1
Kdph1 = 25 #microMol
kph1 = 3
Kph1 = 0.1
k1 = 10
K1 = 1.01
p0 = 0.083 #min-1
delt0 = 0.2
Vr = 10 #volume ratio
p1 = 0.04
delt1 = 0.16 #min-1
kSm = 0.005 # microMol min-1
kSpm = 1
KSpm = 0.1
p2 = 0.083
delt2 = 0.0001
ktm = 1
ks = 0.015
p5 = 0.04
delt5 = 0.2
kSw = 0.003
kSpw = 1
KSpw = 0.1
p6 = 0.083
delt6 = 0.001
ktw = 1
kdph2 = 96
Kdph2 = 26
kph2 = 1
Kph2 = 0.1
E = 0.1
ATMt = 1.3

#Initial conditions
s0 = [0,0,0,0,0,0,0,0,0,0,0,0,0,0,0]

#Equations
def du0(t,u0,v0,u1,u3,u4,u5):
    return kdph1*u5*u3/(Kdph1+u3) - k1*u1*u0/(K1+u0) - kph1*u4*u0/(Kph1+u0) - p0*Vr*(u0-v0)

def du1(t,u1,v1):
    return -p1*Vr*(u1-v1) - delt1*u1

def du2(t,u2,u3):
    return kSm + kSpm*(u3**4)/(KSpm**4 +u3**4) - p2*Vr*u2 - delt2*u2

def du3(t,u0,u3,u4,u5):
```

```

    return kph1*u4*u0/(Kph1+u0) - kdph1*u5*u3/(Kdph1+u3)

def du4(t,u4,u5):
    return kph2*E*(ATMt-u4)/(Kph2+0.5*(ATMt-u4)) - 2*kdph2*u5*(u4**2)/(Kdph2+u4**2)

def du5(t,u5,v5):
    return p5*Vr*v5 - delt5*u5

def du6(t,u3,u6):
    return kSw + kSpw*(u3**4)/(KSpw**4 +u3**4) - p6*Vr*u6 - delt6*u6

def dv0(t,u0,v0,v1):
    return ks - k1*v1*v0/(K1+v0) - p0*(v0-u0) - delt0*v0

def dv1(t,u1,v1,v2):
    return ktm*v2 - p1*(v1-u1) - delt1*v1

def dv2(t,u2,v2):
    return p2*u2 - ktm*v2 - delt2*v2

def dv3(t):
    return 0

def dv4(t):
    return 0

def dv5(t,v5,v6):
    return ktw*v6 - p5*v5 - delt5*v5

def dv6(t,u6,v6):
    return p6*u6 - ktw*v6 - delt6*v6

def system(t, y):
    u0 = y[0]
    u1 = y[1]
    u2 = y[2]
    u3 = y[3]
    u4 = y[4]
    u5 = y[5]
    u6 = y[6]
    v0 = y[7]
    v1 = y[8]
    v2 = y[9]
    v3 = y[10]
    v4 = y[11]
    v5 = y[12]
    v6 = y[13]
    return [du0(t,u0,v0,u1,u3,u4,u5), du1(t,u1,v1), du2(t,u2,u3), \
            du3(t,u0,u3,u4,u5), du4(t,u4,u5), du5(t,u5,v5), du6(t,u3,u6), \
            dv0(t,u0,v0,v1), dv1(t,u1,v1,v2), dv2(t,u2,v2), \
            dv3(t), dv4(t), dv5(t,v5,v6), dv6(t,u6,v6)]

#Time scale
t = np.linspace(0,300,1000)

#Solve
sols = odeint(system, y0=s0, t=t, tfirst=True)

u0 = sols[:,0] #p53(n)

```



```

u1 = sols[:,1] #Mdm2(n)
u2 = sols[:,2] #Mdm2 mRNA (n)
u3 = sols[:,3] #p53-p (n)
u4 = sols[:,4] #ATM-p (n)
u5 = sols[:,5] #Wip1 (n)
u6 = sols[:,6] #Wip1mRNA (n)
v0 = sols[:,7] #p53(c)
v1 = sols[:,8] #Mdm2(c)
v2 = sols[:,9] #Mdm2 mRNA (c)
v3 = sols[:,10] #p53-p (c)
v4 = sols[:,11] #ATM-p (c)
v5 = sols[:,12] #Wip1 (c)
v6 = sols[:,13] #Wip1mRNA (c)

#Plot
plt.plot(t,u0, label = "p53 (n)")
plt.plot(t,u1, label = "Mdm2 (n)")
#plt.plot(t,u2, label = "Mdm2-mRNA (n)")
plt.plot(t,u3, label = "p53-p (n)")
plt.plot(t,u4, label = "ATM-p (n)")
plt.plot(t,u5, label = "Wip1 (n)")
#plt.plot(t,u6, label = "Wip1-mRNA (n)")
plt.plot(t,v0, label = "p53 (c)")
plt.plot(t,v1, label = "Mdm2 (c)")
#plt.plot(t,v2, label = "Mdm2-mRNA (c)")
plt.plot(t,v3, label = "p53-p (c)")
plt.plot(t,v4, label = "ATM-p (c)")
plt.plot(t,v5, label = "Wip1 (c)")
#plt.plot(t,v6, label = "Wip1-mRNA (c)")
plt.ylabel("Concentration (dimensionless)")
plt.xlabel("Time (dimensionless)")
#plt.title("Negative Feedback Model")
plt.legend()
plt.show()

plt.plot(t,u0+u3, label = "Total p53")
plt.plot(t,u1, label = "Mdm2")
#plt.plot(t,u3, label = "p53-p")
plt.plot(t,u4, label = "ATM-p")
plt.plot(t,u5, label = "Wip1")
plt.ylabel("Concentration (dimensionless)")
plt.xlabel("Time (dimensionless)")
plt.title("Nucleus")
plt.legend()
plt.show()

plt.plot(t,v0, label = "p53 (inactive)")
plt.plot(t,v1, label = "Mdm2")
#plt.plot(t,v3, label = "p53-p")
plt.plot(t,v4, label = "ATM-p")
plt.plot(t,v5, label = "Wip1")
plt.ylabel("Concentration (dimensionless)")
plt.xlabel("Time (dimensionless)")
plt.title("Cytoplasm")
plt.legend()
plt.show()

```

Appendix B: Compartmental Model Parameters

Table B-1: Compartmental model parameters

Parameter	Value [Units]	Description
k_{dph1}	$78 \text{ [min}^{-1}\text{]}$	Wip1-dependent p53 dephosphorylation velocity
K_{dph1}	$25 \text{ [}\mu\text{M}\text{]}$	Mich.-Men. rate of Wip1-dependent p53 dephosphorylation
k_{ph1}	$3 \text{ [min}^{-1}\text{]}$	p53 phosphorylation velocity
K_{ph1}	$0.1 \text{ [}\mu\text{M}\text{]}$	Mich.-Men. rate of p53 phosphorylation
k_1	$10 \text{ [min}^{-1}\text{]}$	p53 ubiquitination velocity
K_1	$1.01 \text{ [}\mu\text{M}\text{]}$	Mich.-Men. rate of p53 ubiquitination
P_0	$0.083 \text{ [min}^{-1}\text{]}$	p53 permeability
δ_0	$0.2 \text{ [min}^{-1}\text{]}$	p53 degradation rate
V_r	10 [adim]	Volume ratio
P_1	$0.04 \text{ [min}^{-1}\text{]}$	Mdm2 permeability
δ_1	$0.16 \text{ [min}^{-1}\text{]}$	Mdm2 degradation rate
k_{sm}	$0.005 \text{ [}\mu\text{M min}^{-1}\text{]}$	Basal Mdm2 mRNA transcription rate
k_{sym}	$1 \text{ [}\mu\text{M min}^{-1}\text{]}$	Mdm2 mRNA transcription velocity
K_{sym}	$0.1 \text{ [}\mu\text{M}\text{]}$	Mich.-Men. rate of Mdm2 mRNA transcription
P_2	$0.083 \text{ [min}^{-1}\text{]}$	Mdm2 mRNA permeability
δ_2	$0.0001 \text{ [min}^{-1}\text{]}$	Mdm2 mRNA degradation rate
k_{m2}	$1 \text{ [min}^{-1}\text{]}$	Mdm2 translation rate
k_s	$0.015 \text{ [}\mu\text{M min}^{-1}\text{]}$	Basal p53 synthesis rate
P_5	$0.04 \text{ [min}^{-1}\text{]}$	Wip1 permeability
δ_5	$0.2 \text{ [min}^{-1}\text{]}$	Wip1 degradation rate
k_{sw}	$0.003 \text{ [}\mu\text{M min}^{-1}\text{]}$	Basal Wip1 mRNA transcription rate
k_{syw}	$1 \text{ [}\mu\text{M min}^{-1}\text{]}$	Wip1 mRNA transcription velocity
K_{syw}	$0.1 \text{ [}\mu\text{M}\text{]}$	Mich.-Men. rate of Wip1 mRNA transcription
P_6	$0.083 \text{ [min}^{-1}\text{]}$	Wip1 mRNA permeability
δ_6	$0.001 \text{ [min}^{-1}\text{]}$	Wip1 mRNA degradation rate
k_{w1}	$1 \text{ [min}^{-1}\text{]}$	Wip1 translation rate
k_{dph2}	$96 \text{ [min}^{-1}\text{]}$	Wip1-dependent ATM dephosphorylation velocity
K_{dph2}	$26 \text{ [}\mu\text{M}\text{]}$	Mich.-Men. rate of Wip1-dependent ATM dephosphorylation
k_{ph2}	$1 \text{ [min}^{-1}\text{]}$	ATM phosphorylation velocity
K_{ph2}	$0.1 \text{ [}\mu\text{M}\text{]}$	Mich.-Men. rate of ATM phosphorylation
E	$0.1 \text{ [}\mu\text{M}\text{]}$	Concentration of 'the damage signal'
ATM_{TOT}	$1.3 \text{ [}\mu\text{M}\text{]}$	Total ATM concentration